Iranian Journal of Physics Research, Vol. 24, No. 3, 2024
DOI: 10.47176/ijpr.24.3.11823

Simulating the interactions between the produced neutrons from piezoelectric rocks and the surrounding medium during earthquakes

A Bahari* and S Mohammadi
Department of Physics, Payame Noor University, Tehran, Iran,

E-mail: aboozar.bahari@gmail.com
mohammadi@pnu.ac.ir

(Received 15 January 2024 ; in final form 28 April 2024)

Abstract
Many studies have shown that during earthquakes (EQs), the fracturing of piezoelectric rocks like granite causes atomic/ nuclear particles' radiation into the Earth's crust. With the help of an MCNPX simulation code, we have already studied the amount and energies of created atomic/ nuclear particles and the possible interactions for under-stressed piezoelectric blocks. In this research, applying the PACE4 code, we simulated the interactions between the created neutrons from under-stressed piezoelectric rocks and the elements of granite plus the elements of fractures' filling fluids like water, air, methane, and CO_2, to study the mechanism of such reactions and find which new elements might be produced. The results indicate that compound nuclear reactions like fusion/ fission/ inelastic scattering can happen, resulting in the release of energy from the depths of the Earth in the aseismic regions. Furthermore, compound nuclear interactions from the piezoelectric effect can generate carbon (C), oxygen (O), hydrogen (H), and Nitrogen (N) in the granitic rocks' medium or inside the fracture-filling fluids and trigger the life chain and/or the hydrocarbon chain (oil and gas), inside the Earth's crust of the aseismic regions. It can also result in the production of CO_2 gas. Moreover, in this process, some new elements like Al, Mg, etc., might also be produced in the texture of granitic rocks. In addition, we have found that the increasing amount of nuclear particles and radioactive elements on the surface could be a sign of an incoming earthquake. Besides, neutron capturing might happen between neutrons and the hydrogen nuclei of the underground water, causing the production of deuterium. As a result, an increase in the amount of stable deuterium in the water around the aseismic regions can be a precursor of earthquakes.

Keywords: PACE4, particles' radiation, neutron, granite rocks, piezoelectricity, earthquake

1. Introduction

Up to now, many studies have been performed on particle radiations before or during earthquakes (EQs). Fu et al. found anomalous variations in the gamma-ray counting rate a few days before some local EQs in eastern Taiwan [1]. Maksudov et al. proposed a new method for EQ forecasting, based on simultaneous recording of the intensity of fluxes of low-energy neutrons and charged particles by detectors [2]. Sigaeva et al. observed neutron emission before the Sumatra EQ in Dec. 2004 [3]. Guo et al. analyzed the characteristic response of gamma radiation monitoring to seismic activity. The gamma radiation monitoring in Changsha indicates that near-field EQ swarm or violent EQ affects the gamma radiation in the aseismic region [4].

Carpinteri et al. performed some experimental tests on brittle rock specimens, especially piezoelectric rocks like granite, to check the neutron emission under different kinds of compression tests and monotonic, cyclic, and ultrasonic mechanical loading [5-9]. Manuelo et al. also performed neutron emission measurements on granite specimens from Sardinia during mechanical compression tests [10].

Bahari et al., with the help of piezoelectricity relationships and the elastic energy formula, applied the MCNPX simulation code to find the amount of created atomic/ nuclear particles, the dominant interactions, and the possible particle energies for various sizes of quartz and granite blocks. They have proved that for the large granite blocks, "photonuclear" interactions from the "Bremsstrahlung gamma ray" photons due to the Relativistic Run-Away Electron Avalanche (RREA), is the main mechanism for nuclear particle creation when the stress is exerted on a large piezoelectric block. In addition, they have presented some formulas to estimate the quantity and energy of various created particles on a fracture surface, when the piezoelectric block is under different uniaxial stress. They have also simulated the flux of the particles, created from under-stressed granitic rocks at different distances from the EQ hypocenter inside the fractures, filled with air, water, and CO_2 [11, 12].

In addition, some researches indicate that during seismic activities, due to some kinds of nuclear interactions, new elements might be produced. Jones et al. suggested that the fusion of deuterium and hydrogen could produce the isotope helium-3 deep inside the Earth. This mechanism

would also explain the high levels of helium-3 found in rocks, liquids, and gases from volcanoes and regions in the Earth's crust where tectonic plates are active. Jones and his group said that the tritium detected in the gases from volcanoes is further evidence of cold fusion [13]. Besides, Palmer proposed that there is a correlation between the heat and the helium-3 found in volcanoes and that this might be due to the fusion. He suggested that the fusion is a possible and likely explanation for several geologic phenomena [14]. Carpinteri et al. suggested that the low-energy nuclear reactions from active faults could be considered as a relevant cause of carbon formation and degassing of freshly-formed CO_2 during seismic activity [15]. Tamburello et al. used an ad-hoc point pattern analysis to show that there is a spatial correlation between CO_2 discharges and the presence of active fault systems [16].

The elemental changes due to the fracturing or pressure application on materials were the subject of some other research. Cardone et al. have applied ultrasonic waves to cylindrical bars of steel and alpha-iron (ferrite), resulting in the emission of neutron bursts and producing several roughly circular dark regions with diameters of a few millimeters on the bar surfaces [17, 18]. Albertini et al. made a chemical investigation of structural damage produced by the exposure of an iron bar to ultrasound pressure waves. They have shown that the material in the micro-cavities shows a systematic increase in carbon (C), chromium (Cr), and manganese (Mn), and a decrease in iron (Fe) [19].

It must be taken into account that the cracks/ fractures are generated inside the blocks of rocks before the EQ happens, because of the mechanical stresses, applied on them. Fractures might be filled with fluids like air, oil, gas, water, CO_2, etc. and in this situation, the type and state of the fluid (liquid or gas) can make a large difference in the response of the seismic waves [20].

Another point that should be taken into account is that since the neutrons do not have an electric charge, they freely penetrate through the electron shells of atoms and are not repelled by the Coulomb field of the nucleus [21]. Hence, they are proper particles to study their interactions with other material elements.

In this research, with the help of a Monte Carlo code, we want to simulate the interactions between the created neutrons from under-stressed granite rocks and the elements of granite plus the elements of fractures' filling fluids like water, air, methane, and CO_2 to study the mechanism of such reactions and to find which new elements might be produced from the compound nucleus reactions. The importance of this simulation is to prove that some elements and/ or chemical compounds, playing a big role in the life chain, like O, H, C, N, F, and hydrocarbons (oil/ gas), can be generated from piezoelectricity phenomena deep inside the Earth, before or during the EQs. In addition, the effect of EQ magnitude on the production and diversity of new elements/ compounds will be analyzed.

2. Materials and methods

2.1 Compound nucleus reactions

In compound nucleus reactions an incident particle enters a target nucleus with an impact parameter small, compared with the nuclear radius. It then will have a high probability of interacting with one of the nucleons of the target, possibly through a simple scattering. The recoiling struck nucleon and the incident particle (now with less energy) can each make successive collisions with other nucleons and after several such interactions, the incident energy is shared among many of the nucleons of the combined system of projectile + target. The average increase in energy of any single nucleon is not enough to free it from the nucleus, but as many more-or-less random collision occurs, there is a statistical distribution in energies and a small probability for a single nucleon to gain a large enough share of the energy to escape. Much as molecules evaporate from a hot liquid [22].

As an example for a compound nucleus, the reaction between a projectile neutron and ^{27}Al, depending on the neutron's energy, an excited compound nucleus can be formed in the following sets and final products are produced, independent of the means of formation of the compound nucleus

$$n + {}^{27}_{13}Al \rightarrow {}^{28}_{13}Al^{*} \rightarrow {}^{27}_{13}Al + n + \gamma$$

$$n + {}^{27}_{13}Al \rightarrow {}^{28}_{13}Al^{*} \rightarrow {}^{27}_{12}Mg + p + \gamma$$

The decay probability depends only on the total energy given to the system; in fact, the compound nucleus "forgets" the process of formation and decays governed primarily by statistical rules. Another characteristic of compound-nucleus reactions is the angular distribution of the products [22].

2.2. Introduction to PACE4 simulation code

The code PACE (Projection Angular-momentum Coupled Evaporation) uses a Monte Carlo method and has been incorporated in the LISE++ package [23-25]. This code is based on the Hauser-Feshbach theory of compound nucleus (CN) decay and uses the statistical approach of CN de-excitation by Monte Carlo procedure. The code calculates at each stage of de-excitation, the angular momentum projection which enables the determination of angular distributions of the emitted particles [26]. This code uses the BASS model to calculate the fusion cross sections [27]. Besides, this code can calculate a fusion cross section below the Coulomb barrier using the quantum-mechanical approach [28]. The AME2003 database of recommended values [29] for binding energies can be used in the calculations.

2.3. Assumptions of the problem for simulation with PACE4

Granite is a common type of igneous rock, which is characterized by a high concentration in the rocks that make up the Earth's crust (about 60 % of the Earth's crust). As already we have studied (reference [11]), for a typical granite rock with the elemental percentage as shown in table 1, the piezoelectric coefficient (d) equals 7×10^{-13} C/N (at room temperature) [30], relative permittivity (ϵ_r) equals to 5 [31] and the uniaxial compressive strength of 140 MPa when the compressive stress is applied on various sizes of rock block, some atomic/ nuclear particles are released from the rock medium [11].

Table 1. A typical elemental percentage of granite, based on its chemical composition [11].

Elements	O	Si	Al	K	Na	Ca	Fe	Total
Percentage, %	62	22.5	9	3	2	0.5	1	**100**

Table 2. The computed initial energy of the radiated runaway electrons and the estimated average energy of the created particles inside the granite rock tissue, achieved from the simulation outputs in NPS electron= 1000 for two M_L [11].

Block dimensions,m^3	M_L	Initial runaway electrons' energy, MeV	The average energy of the created particles, MeV			
			Neutrons (n)	Photons (γ)	Electrons (e)	Protons (p)
400^3	**5.79**	885	10.4	1.81	0.03	9.38
4000^3	**7.67**	8858	24.6	3.05	0.04	20

Table 3. Simulation results with PACE4 for the interactions between neutrons with $E_n = 0$ and the target nuclei.

Projectile	Target	Fusion radius, fm	Barrier height, MeV	Q-value of reaction, MeV	Yields of residual nuclei	Percent, %	x-section, mb	Reaction
n	**^{1}H**	0	0	2.225	**^{2}H (D)**	100	1.00E+20	^{1}H (n,γ) D
n	**^{16}O**	0	0	4.143	**^{17}O**	100	1.00E+20	^{16}O (n,γ) ^{17}O
n	**^{28}Si**	0	0	8.474	**^{29}Si**	100	1.00E+20	^{28}Si (n,γ) ^{29}Si
n	**^{27}Al**	0	0	7.725	**^{28}Al**	100	1.00E+20	^{27}Al (n,γ) ^{28}Al
n	**^{12}C**	0	0	4.946	**^{13}C**	100	1.00E+20	^{12}C (n,γ) ^{13}C
n	**^{14}N**	0	0	4.946	**^{15}N**	100	1.00E+20	^{14}N (n,γ) ^{15}N

As investigated in our previous research, the initial energy of the runaway electrons, emitted inside the granite rock medium can be calculated, by applying the piezoelectric and elastic energy relationships. The average energy of the created particles can be estimated, using the MCNPX simulation. In this code, the cell card was defined with side lengths of 40 m, 400 m, and 4000 m for three large granite cubic blocks. In the material card, the elements of the chemical composition of granite with their percentage were provided to the code. In the source card, the electrons were selected as the source particle (runaway electrons) because of the voltage, generated from the piezoelectric effect, and their position was selected as a surface source on the left side of the block (figure 6 of the Ref. [11]). Their energy, given to the code for simulation was the computed initial energy of the runaway electrons from piezoelectric equations and elastic energy relations (eqs. 1- 15 of Ref. [11]).

Table 2 reveals the computed initial energy of the runaway electrons and the estimated average energy of the created particles inside the granite rock, obtained from the simulation outputs for number of electrons (NPS electron) = 1000 for two EQ Richter magnitudes (M_L) [11].

3. Results and discussions

3.1. Simulation of nuclear interactions between created neutrons and the main elements of granite, water, air, carbon dioxide (CO_2) and methane (CH_4)

To simulate the nuclear interactions when created neutrons from the piezoelectric effect collide with the other atoms' nuclei, we employed the PACE4 code, its methodology was already explained in section 2.2. It must be taken into account that since the neutrons are neutral-charged particles, even very low-energy neutrons will interact with the other nuclei. Hence, we first considered the neutrons with energy equal to zero, and then, neutrons with average E_n equal to 10.4 and 24.6 MeV (for the earthquake with the M_L= 5.79 and 7.67, respectively) were taken into account.

As shown in table 1, the main granite elements are ^{16}O, ^{28}Si, and ^{27}Al. Hence, our simulation was run only for these elements. In addition, inside the cracks/fractures of the Earth's crust, sometimes air, water, CO_2, and CH_4 are present, possessing mainly elements of ^{1}H, ^{16}O, ^{14}N, and ^{12}C; these elements were selected, too, for our simulation. Table 3 indicates the simulation results with PACE4 for the interactions between a neutron with $E_n = 0$ and the target nuclei. As can be seen in this table, for $E_n = 0$, yields of residual nuclei illustrate that for all of the interactions, neutron capturing occurs, leading to stable nuclei production that possesses a mass number one more than before. The reaction between neutron and hydrogen, resulting in the production of deuterium, is so important because increasing the amount of deuterium in the water around the aseismic regions can be a precursor of incoming earthquakes.

Furthermore, for $E_n = 0$, the fusion radius in fm and barrier height in MeV is zero for all reactions. Besides, the cross-section (x-section) in mb is too high (1.00E+20) for all interactions. The released energy (Q-value of reaction) in MeV for each of these interactions has different values which can be found in table 3.

Tables 4 and 5 indicate the simulation results with PACE4 for the interactions between neutrons with E_n = 10.4 and 24.6 MeV; and the target nuclei. Figures 1 to 6 illustrate the cross-section of the produced isotopes for the compound nucleus reaction between an incident neutron and ^{1}H, ^{16}O, ^{28}Si, ^{27}Al, ^{12}C, and; ^{14}N, respectively, in E_n = 24.6 MeV.

Table 4. Simulation results with PACE4 for the interactions between neutrons with E_n = 10.4 MeV and the target nuclei.

Projectile	Target	Fusion radius, fm	Barrier height, MeV	Q-value of reaction, MeV	Yields of residual nuclei	Percent, %	x-section, mb	Reaction
n	**^{1}H**	1.1	0	2.225	**^{2}H (D)**	100	90.57	^{1}H (n,γ) D
n	**^{16}O**	2.95	0	4.14	**^{17}O**	0.1	0.1	^{16}O (n,γ) ^{17}O
					^{16}O	74.8	448	^{16}O (n,n) ^{16}O
					^{13}C	25.1	150	^{16}O (n,α) ^{13}C
n	**^{28}Si**	3.6	0	8.47	**^{28}Si**	90.3	821	^{28}Si (n,n) ^{28}Si
					^{25}Mg	9.70	88.2	^{28}Si (n,α) ^{25}Mg
n	**^{27}Al**	3.55	0	7.72	**^{27}Al**	97.5	862	^{27}Al (n,n) ^{27}Al
					^{27}Mg	2.5	22.1	^{27}Al (n,D) ^{27}Mg
n	**^{12}C**	2.65	0	4.94	**^{13}C**	4.3	20.7	^{12}C (n) ^{13}C
					^{12}C	20.4	98.4	^{12}C (n,n) ^{12}C
					^{9}Be	75.3	363	^{12}C (n,α) ^{9}Be
n	**^{14}N**	2.8	0	10.83	**^{14}N**	27.7	150	^{14}N (n,n) ^{14}N
					^{14}C	20.1	109	^{14}N (n,p) ^{14}C
					^{11}B	52.2	282	^{14}N (n,α) ^{11}B

As can be understood from tables 3, 4, and 5, some of the produced isotopes are radioactive and they will decay by radiating particles during the time to reach a stable mode. Those particles also can reach the surface via the fractures/ cracks of the rocks and be detected by the surface/ nearby wells' detectors [12]. As a result, the increasing amount of nuclear particles and radioactive elements on the surface is a sign of an incoming earthquake.

In addition, as can be found in tables 4 and 5, some new elements like Al, Mg, etc, that do not exist in the normal granite composition, might be produced in the medium of this rock; as a result of the nuclear interactions from the piezoelectric effect in aseismic regions.

Furthermore, figure 6 and 7 show the plotted cross-section of the capturing reaction for n+ ^{1}H → ^{2}H + Q (2.225 MeV) and for ^{28}Si (n,γ) ^{29}Si within various energy ranges of the neutron, respectively. These figures were plotted from the ENDF Library of Nuclear Data Services [32]. As could be seen in these figures, as the incident neutron energy increases, the cross-section of the capturing reaction, decreases, and thence, lower energy neutrons are more competent for neutron capturing reaction, releasing energy (Q-value of reaction). Figure 8 represents the plotted cross-section of inelastic scattering for ^{28}Si (n, p) ^{28}Al within various energy ranges of neutrons.

4. Conclusion

- The compound nucleus reaction between the created neutrons and the elements of granite and fracture's filling fluids can lead to the release of energy (Q-value) from depths of the Earth in the aseismic regions where stress is applied on the piezoelectric rocks. This heat, itself, results in more mechanical stress generation in these regions. In addition, some of the produced isotopes are radioactive with short or long half-lives and they will emit new particles during their decay periods. Hence, these radiations are the secondary products of the seismic activities that provide the energy for the Earth. As a result:
- The increasing amount of nuclear particles and radioactive elements on the surface is a sign of an incoming earthquake.
- Neutron capturing might happen between neutrons and the hydrogen nuclei of the underground water, causing the production of deuterium. As a result, an increase in the amount of stable deuterium in the water around the aseismic regions can be a precursor of earthquakes.
- Compound nuclear interactions from the piezoelectric effect can generate carbon (C), oxygen (O), hydrogen (H), and Nitrogen (N) in the granitic rocks' medium or inside the fracture-filling fluids and trigger the life chain in the presence of water and/or the hydrocarbon chain (oil and gas), deep inside the Earth's crust of the aseismic regions. Besides, it can result in the production of CO_2 gas in agreement with earlier works such as ref. 14 and 15 and the generation of hydrocarbons (oil and gas).
- Some new stable elements like Al, Mg, etc, being not present in common granite composition, might be produced in the texture of this rock, due to the nuclear interactions from the piezoelectric effect in aseismic zones.
- As the earthquake magnitude is increased, the diversity of the newly produced elements in the granitic rock medium and the fractures' filling fluids will be raised.
- Another kind of stable or unstable isotopes can be created due to the interactions between the neutrons and the other types of igneous, metamorphic, or sedimentary rocks like basalt, carbonates, shales, etc; due to the nuclear interactions from the piezoelectric effect in aseismic zones.

Table 5. Simulation results with PACE4 for the interactions between neutrons with E_n = 24.6 MeV and the target nuclei.

Projectile	Target	Fusion radius, fm	Barrier height, MeV	Q-value of reaction, MeV	Yields of residual nuclei	Percent, %	x-section, mb	Reaction
n	**^{1}H**	1.1	0	2.225	**^{2}H (D)**	100	57.2	^{1}H (n,γ) D
n	**^{16}O**	2.95	0	4.14	**^{16}O**	28.2	116	^{16}O (n,n) ^{16}O
					^{16}N	0.1	0.41	^{16}O (n,p) ^{16}N
					^{15}O	9.5	39.1	^{16}O (n,2n) ^{15}O
					^{15}N	30	123	^{16}O (n,D) ^{15}N
					^{13}C	5.8	23.9	^{16}O (n,α) ^{13}C
					^{12}C	22.1	90.9	^{16}O (n,n+α) ^{12}C
					^{9}Be	4.3	17.7	^{16}O (n, 2α) ^{9}Be
n	**^{28}Si**	3.6	0	8.47	**^{28}Si**	12.7	78.6	^{28}Si (n,n) ^{28}Si
					^{28}Al	5.5	34	^{28}Si (n,p) ^{28}Al
					^{27}Si	6	37.1	^{28}Si (n,2n) ^{27}Si
					^{27}Al	64.9	402	^{28}Si (n,D) ^{27}Al
					^{27}Mg	1.2	7.4	^{28}Si (n,2p) ^{27}Mg
					^{25}Mg	4.8	29.7	^{28} Si (n,α) ^{25}Mg
					^{24}Mg	0.4	2.4	^{28}Si (n,n+α) ^{24}Mg
					^{21}Ne	4.5	27.9	^{28}Si (n,2α) ^{21}Ne
n	**^{27}Al**	3.55	0	7.72	**^{27}Al**	13.1	78.8	^{27}Al (n,n) ^{27}Al
					^{27}Mg	6.6	39.7	^{27}Al (n,D) ^{27}Mg
					^{26}Al	29.1	175	^{27}Al (n,2n) ^{26}Al
					^{26}Mg	16.3	98.1	^{27}Al (n,D) ^{26}Mg
					^{24}Na	1.9	11.4	^{27}Al (n,α) ^{24}Na
					^{23}Na	32.1	193	^{27}Al (n,n+α) ^{23}Na
					^{23}Ne	0.9	5.4	^{27}Al (n,p+α) ^{23}Ne
n	**^{12}C**	2.65	0	4.94	**^{12}C**	75	248	^{12}C (n,n) ^{12}C
					^{12}B	0.3	0.9	^{12}C (n,p) ^{12}B
					^{11}C	3	9.9	^{12}C (n,2n) ^{11}C
					^{11}B	10.1	33.4	^{12}C (n,D) ^{11}B
					^{9}Be	9.5	31.4	^{12}C (n,α) ^{9}Be
					^{5}He	1.1	3.6	^{12}C (n,2α) ^{5}He
n	**^{14} N**	2.8	0	10.83	**^{14}N**	5.1	18.9	^{14}N (n,n) ^{14}N
					^{14}C	3.6	13.3	^{14}N (n,p) ^{14}C
					^{13}N	12.6	46.6	^{14} N (n,2n) ^{13}N
					^{13}C	57.7	214	^{14} N (n,D) ^{13}C
					^{12}C	0.1	0.37	^{14} N (n,n+D) ^{12}C
					^{11}B	3.7	13.7	^{14}N (n,α) ^{11}B
					^{10}Be	1.2	4.4	^{14}N (n,p+α) ^{10}Be
					^{7}Li	15.7	58.1	^{14}N (n,2α) ^{7}Li

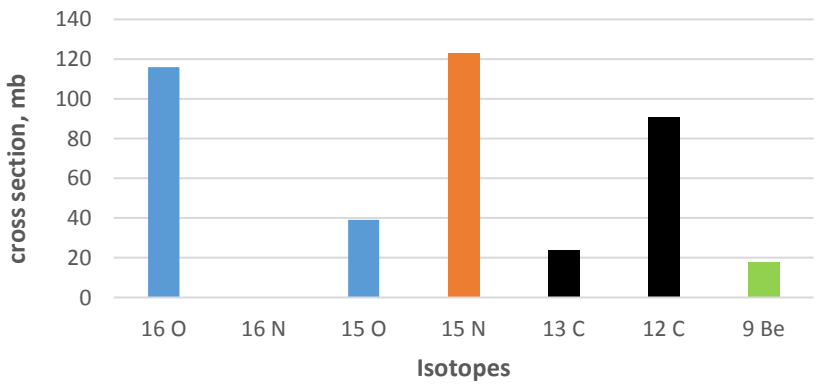

Figure 1. Cross section of the produced isotopes for the reaction between an incident neutron and ^{16}O in E_n = 24.6 MeV.

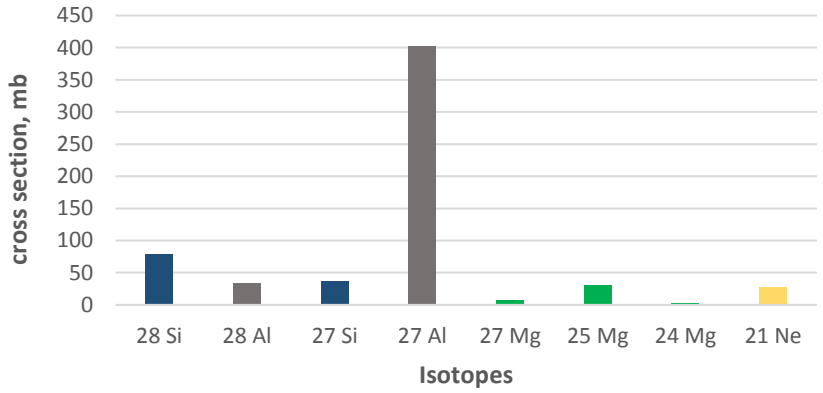

Figure 2. Cross section of the produced isotopes for the reaction between an incident neutron and ^{28}Si in E_n = 24.6 MeV.

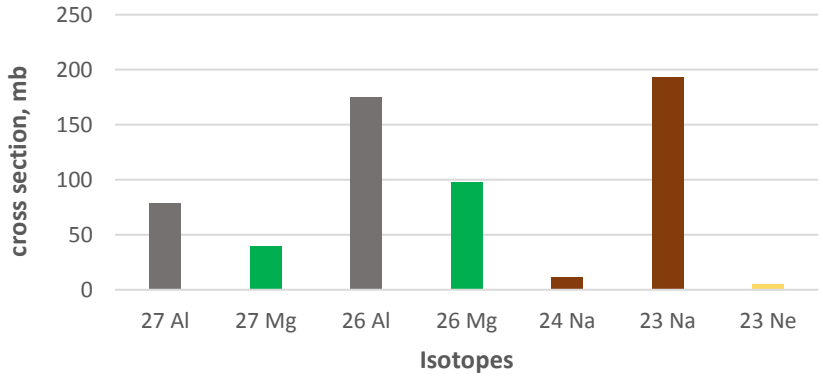

Figure 3. Cross section of the produced isotopes for the reaction between an incident neutron and ^{27}Al in E_n = 24.6 MeV.

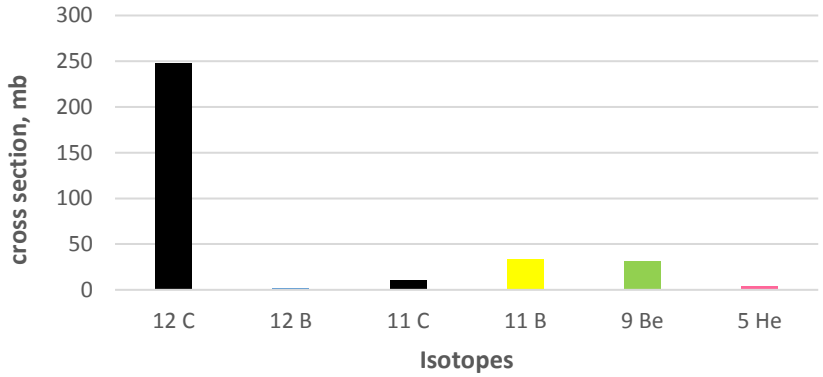

Figure 4. Cross section of the produced isotopes for the reaction between an incident neutron and ^{12}C in E_n = 24.6 MeV.

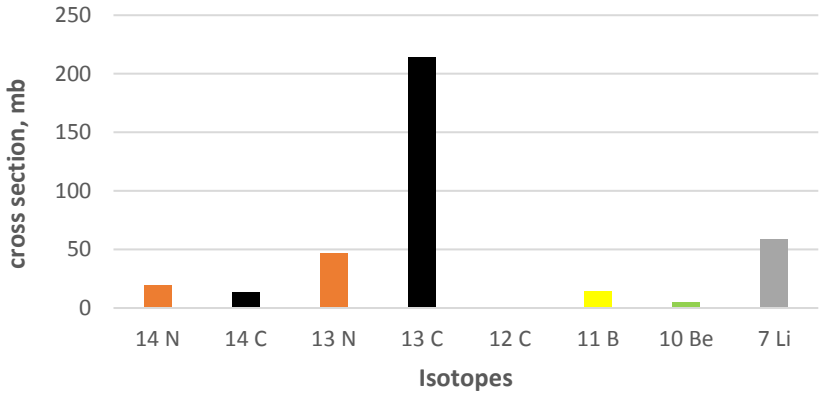

Figure 5. Cross section of the produced isotopes for the reaction between an incident neutron and ^{14}N in E_n = 24.6 MeV.

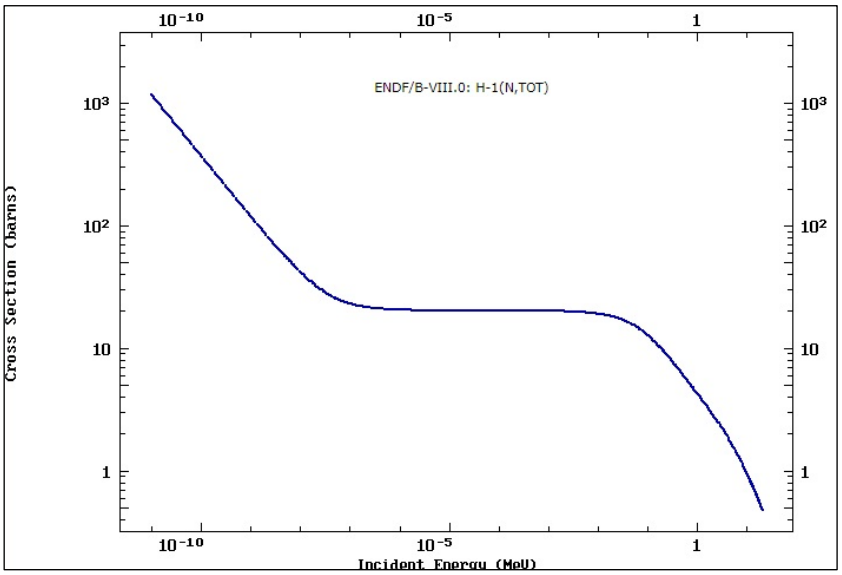

Figure 6. Cross section of capturing reaction for n+ $^{1}H \rightarrow {}^{2}H$ + 2.225 MeV within various energy ranges of the neutron.

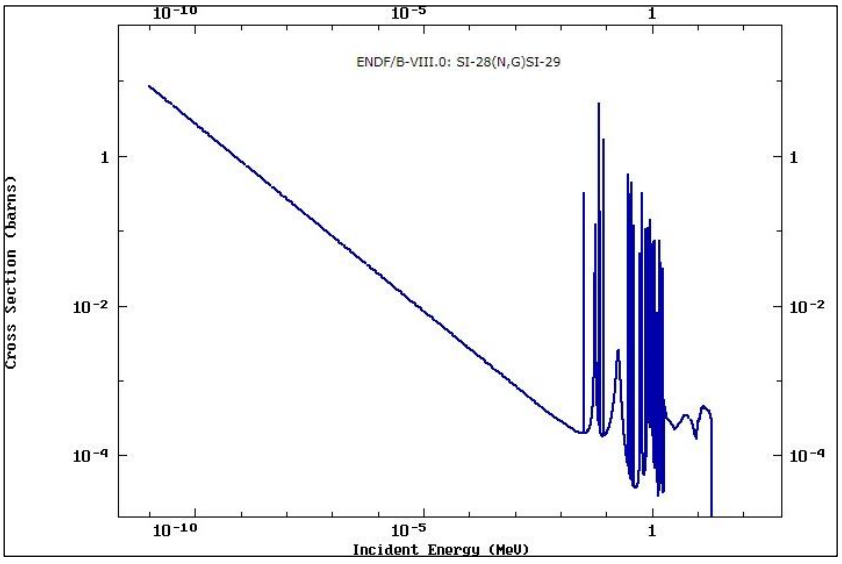

Figure 7. Cross section of capturing reaction for ^{28}Si (n,γ) ^{29}Si within various energy ranges of the neutron.

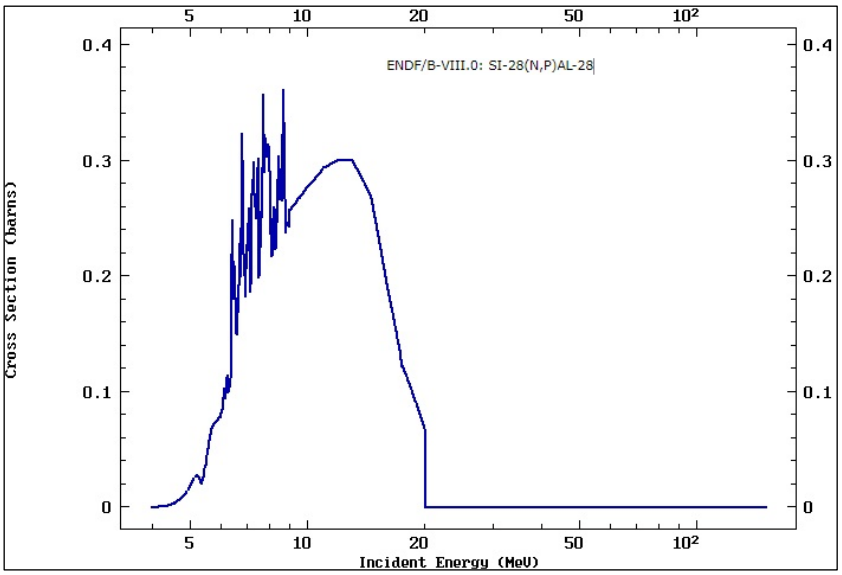

Figure 8. Cross section of inelastic scattering for ^{28}Si (n, p) ^{28}Al within various energy ranges of the neutron.

Data availability statement

The data that support the findings of this study are available from the corresponding author upon reasonable request.

Funding and/or Conflicts of interests/Competing interests

There is no funding for this research.

There are no conflicts of interest for this research.

References

1. C C Fu, et al., *J. Asian Earth Sci*. **114**, 2 (2015) 362.
2. A U Maksudov and M A Zufarov, *EQ Sci*. **30**, 5-6 (2017) 283.
3. E Sigaeva et al., *Geophys. Res. Abstr*. **8** (2006) 00435.
4. X Guo, J Yan, and Q Wang, *J. Environ. Radioact*. **213** (2020) 106119.
5. A Carpinteri, F Cardone, and G Lacidogna, *Strain* **45** (2009) 332.
6. F Cardone, A Carpinteri, and G Lacidogna, *Phys. Lett.* A **373** (2009) 4158.
7. A Carpinteri, F Cardone, and G Lacidogna, *Exp. Mech*. **50** (2010) 1235.
8. A Carpinteri, et al., *Phys. Mesomech*. **13** (2010) 268
9. A Carpinteri, et al., *Strength Fract. Complex*. **7** (2011) 13.
10. A Manuello, B Grosso, and R Ricciu, *Meccanica* **50**, 5 (2014).
11. A Bahari, et al., *Radiat. Eff. Defects Solids* **177**, 7–8 (2022) 743.
12. A Bahari, et al., *At. Indonesia* **1**, 1 (2024) 27.
13. S Jones, S F Taylor, and J Rafelski, *Nature* **338** (1989) 737.
14. E P Palmer, "*AIP Conference Proceedings*" (1991).
15. A Carpinteri and G Niccolini, *Sci*. **1** (2019) 17.
16. G Tamburello, et al., *Nat. Commun.* **9** (2018) 4608.
17. F Cardone, V Calbucci, and G Albertini, *J. Adv. Phys.* **2**, 1 (2013) 20.
18. F Cardone, et al., *Mod. Phys. Lett.* A 27, **18** (2012) 1250102.
19. G Albertini, et al., *Appl. Phys.* A **114**, 4 (2014) 1233.
20. J Berryman, *Geophys. J. Int.* **171** (2007) 954.
21. I Obodovskiy, "*Radiation Fundamentals, Applications, Risks, and Safety*", Elsevier; 1st edition (2019).
22. K S Krane, *"Introductory nuclear physics*", Wiley; 3rd edition (1987).
23. A Gavron, *Phys.Rev.* **C21** (1980) 230.
24. O B Tarasov and D Bazin, *Nucl. Instrum. Methods Phys. Res.* B **204** (2003) 174.
25. O B Tarasov and D Bazin, *Nucl. Instrum. Methods Phys. Res.*, B **266** (2008) 4657.
26. A Sabir, et al., *J. Mod. Phys*. **05** (2014) 18.
27. R Bass, *Phys. Rev. Lett.* **39** (1977) 265.
28. C Y Wong, *Phys. Rev. Lett*. **31** (1973) 766.
29. G Audi, A H Wapstra, and C Thibault, *Nucl. Phys*. A **729**, 1 (2003) 337.
30. T Matsuda, C Yamanaka, and M Ikeya, *Jap. J. Appl. Phys*. **44**, 2 (2005) 968.
31. S S Hubbard, et al., *Lead. Edge* **16**, 11 (1997) 1623.
32. International Atomic Energy Agency (IAEA), "Evaluated Nuclear Data File (ENDF)": https://www-nds.iaea.org/exfor/endf.htm, database version of: (2022-04-22).